HHS Public Access

Author manuscript

Exp Neurol. Author manuscript; available in PMC 2019 June 01.

Published in final edited form as:

Exp Neurol. 2018 June ; 304: 82–89. doi:10.1016/j.expneurol.2018.03.001.

Subacute intranasal administration of tissue plasminogen activator improves stroke recovery by inducing axonal remodeling in mice

Ning Chen, MD, PhD[1,2], **Michael Chopp, PhD**[1,3], **Ye Xiong, MD, PhD**[4], **Jian-Yong Qian, MD, PhD**[1], **Mei Lu, PhD**[5], **Dong Zhou, MD, PhD**[2], **Li He, MD, PhD**[2], and **Zhongwu Liu, MD, PhD**[1]

[1]Department of Neurology, Henry Ford Hospital, Detroit, MI

[2]Department of Neurology, West China Hospital of Sichuan University, Chengdu, Sichuan, P.R. China

[3]Department of Physics, Oakland University, Rochester, MI

[4]Department of Neurosurgery, Henry Ford Hospital, Detroit, MI

[5]Biostatistics and Research Epidemiology, Henry Ford Hospital, Detroit, MI

Abstract

In addition to thrombolysis, tissue plasminogen activator (tPA) can evoke neurorestorative processes. We therefore investigated the therapeutic effect of subacute intranasal administration of tPA post stroke on neurological recovery and on corticospinal innervation in mice. A transgenic mouse line, in which the pyramidal neurons and corticospinal tract (CST) axons are specifically labeled by yellow fluorescent protein (YFP) was employed. Adult CST-YFP mice were subjected to right unilateral middle cerebral artery occlusion (MCAo), and were randomly divided into groups treated with saline or tPA intranasally in the subacute phase. Pseudorabies virus (PRV)-614-monomeric red fluorescent protein (RFP) was injected into the left forelimb. The cervical spinal cord and brain were processed for fluorescent microscopy to detect YFP and RFP labeling. Primary embryonic neurons were cultured with tPA at different concentrations. Neurite length and branch numbers were then measured. In vivo, subacute tPA treatment significantly enhanced functional recovery ($p<0.05$), and increased CST density in the denervated gray matter, and in the numbers of PRV-labeled neurons in bilateral cortices. The behavioral performance was significantly correlated with axonal density in the denervated spinal cord. In vitro, both neurite length and branch numbers significantly increased with concentration of tPA ($p<0.05$). Our results demonstrate that tPA dose-dependently increases neurite outgrowth and branching of cultured

Correspondence to: Zhongwu Liu, MD, PhD, Neurology Research, E&R Bldg., Room 3083, Henry Ford Hospital, 2799 West Grand Boulevard, Detroit, MI 48202, USA, Tel: (313)916-8934 Fax: (313)916-1318 zliu@neuro.hfh.edu, Li He, MD, PhD, Department of Neurology, West China Hospital of Sichuan University, 37 Wainan Guoxue Xiang, Chengdu, Sichuan 610041, P.R. China, Tel: (86 28)85423550 Fax: (86 28)85423550 heli2003new@126.com.

Disclosures

None.

cortical neurons. Subacute intranasal administration of tPA may provide enhance neurological recovery after stroke by promoting CST axonal remodeling.

Keywords

axonal remodeling; functional recovery; middle cerebral artery occlusion; stroke; tissue plasminogen activator

Introduction

Recombinant human tissue plasminogen activator (tPA) remains the only FDA-approved pharmacological therapy and is the mainstay of early treatment of acute ischemic stroke (Jauch et al., 2013; Powers et al., 2015). However, its application is limited by a narrow treatment time window, and side effects of intracranial hemorrhage and brain edema, which may be fatal (Jauch et al., 2013).

Since few neuroprotective agents have proved effective in reducing cerebral infarction and improving neurological functions clinically, and there appears to be strict time limitations for neuroprotective treatment of stroke (Jauch et al., 2013; Powers et al., 2015), we shifted our focus to neurorestorative therapies that could be used in the subacute or chronic phases after stroke and are designed to enhance functional recovery by promoting neuronal plasticity. Most functional impairments after stroke such as hemiparesis are consequences of interruption of neurological electrical signal transmission, so reestablishment of synaptic innervation between cerebral and peripheral nervous systems may provide a physical substrate for functional recovery. Observations from animal models of ischemic stroke have suggested that axonal remodeling of the corticospinal tract (CST), the primary transmission tract from the sensorimotor cortex formed by the long axons of the cortical pyramidal neurons extending to the spinal cord, contribute to neurological recovery, and may provide a treatment target for neurorestorative therapeutic approaches for stroke (Liu et al., 2013; Liu et al., 2009; Zai et al., 2011). Since tPA has oligotrophic and neurotrophic functions and promotes axonal regeneration and brain plasticity in the developing and injured central nervous system (CNS) (Docagne et al., 2015), tPA may also be considered as a promising neurorestorative agent for stroke during the subacute phase. Our preliminary study demonstrated, for the first time, that subacute (7 day post-stroke) tPA intranasal treatment significantly improved sensorimotor functional outcome after ischemic stroke in rats (Liu et al., 2012). However, in this initial study, due to technical limitations, only part of the contralesional CST and corticorubral tract (CRT) were anterogradely labeled. How and why intranasal tPA administration promotes neurorestoration, especially in the denervated spinal cord, and whether the functional benefit directly derives from tPA facilitating CST remodeling remain unclear. Therefore, in the present study we employed a transgenic mouse line, in which the CST axons are specifically and completely labeled by yellow fluorescent protein (YFP), combined with an additional trans-synaptic retrograde pseudorabies virus (PRV) carrying monomeric red florescent protein (RFP) tracing, in order to investigate the anatomical substrate of motor functional recovery after stroke with subacute intranasal administration of tPA. In addition, as a complementary study, we investigated the direct

effect of exogenous tPA on neurite outgrowth in cultured mouse embryonic cortical neurons in vitro.

Methods

Animals

Transgenic CST-YFP mice, in which the cortical neurons in the forebrain and the CST are specifically labeled by YFP, were used in a blinded fashion for functional evaluation and tissue analysis. These mice were generated by an in-house breeding colony of two transgenic mouse strains of B6.Cg-Tg (Thy1-EYFP)15Jrs/J and B6.129-Emx1$^{tm1\ (cre)Krj}$/J purchased from Jackson Laboratories (Bar Harbor, ME, USA) (Bareyre et al., 2005; Liu et al., 2013; Liu et al., 2009). All experimental procedures were approved by the Institutional Animal Care and Use Committee of Henry Ford Hospital.

Animal Model

Adult male CST-YFP mice (n=22; 2–3 month-old; body weight 25–30 g) were subjected to permanent right middle cerebral artery occlusion (MCAo) using a method of intraluminal suture vascular occlusion, modified in our laboratory(Chen et al., 2005). Briefly under isoflurane anesthesia, an 8-0 surgical nylon suture with an expanded silicone tip was advanced from the right external carotid artery (ECA) into the lumen of the internal carotid artery (ICA) to block the origin of the MCA. Two mice died within the first week post-surgery, and the remaining animals were randomly divided into the tPA-treatment group or the control group (n=10/group). Another group of CST-YFP mice (n=10; of comparable age and weight versus the mice in MCAo groups) without surgery were used for normal control.

Intranasal administration of tPA

The mice allocated to the active intervention group were administered 4 doses of tPA (300 ug/dose; Genentech Inc, San Francisco, CA, USA) intranasally at day 7, 9, 11 and 13 after MCAo. The method described by Thorne et al (Thorne et al., 2004) was modified by placing ten 3-μL drops alternately onto each nostril with a 3-min interval between drops which were naturally sniffed in by the mouse placed in a supine and horizontal head position (Liu et al., 2012). The mice were kept in a supine position for an additional 10 min. The same method of administration of the same volume of saline (30 uL in total) was used in the animals of control group. The volume of the dose was determined by the volume of the nasal cavity of the mouse (Gross et al., 1982).

Behavioral Tests

To monitor the neurological functional deficits and recovery, two kinds of tests were performed prior to MCAo, and at 1, 3, and 7 days after MCAo, and weekly thereafter. An adhesive-removal test was applied to detect the sensorimotor deficits after CNS injury; a small quarter-circle adhesive-backed paper dot was placed onto the impaired forepaw, and the time to remove the dot was recorded (Chen et al., 2001). In addition, a single-pellet reaching test was performed to characterize skilled reaching ability of the impaired left forepaw (Farr and Whishaw, 2002; Liu et al., 2013). Animals were trained for 2 weeks before surgery to use their left forepaw to extract 14-mg food pellets (Bio-Serv Inc,

Frenchtown, NJ, USA) through a vertical slot of the front wall. We counted the number of the left forepaw extensions through the slot and the number of pellets extracted, and then recorded the pellet number extracted in a total of 20 attempts. Performance was defined by Percent Success = (number of successful retrievals/20)*100 (Farr and Whishaw, 2002; Liu et al., 2013).

Retrograde PRV tracing

When the behavioral tests were completed at day 28 after MCAo, a retrograde trans-synaptic tracer PRV-614-RFP (Gift from Dr. Lynn Enquist, Princeton University NJ, USA) of a 10 μl total volume was injected into the wrist flexor muscles of the left stroke-impaired forelimb through a skin incision. Then the animals survived 4 additional days in a Biosafety Level-2 facility to allow for virus transport from the muscles to the motor cortices prior to sacrifice (Liu et al., 2009). Mice in the normal control group also received the same dose of PRV-614-RFP injection at 4 days before sacrifice.

Tissue preparation

The mice were sacrificed 4 days after PRV injection and then perfused with saline, followed by 4% paraformaldehyde. The entire brain and the cervical cord were immersed in paraformaldehyde overnight. The brain was cut into 100 μm-thick coronal sections by using a vibratome machine. A series of sections with 900 μm intervals were stained with hematoxylin and eosin (H&E) to measure ischemic lesion volume. A series of sections were processed for Prussian blue staining (ferric hexacyanoferrate and hydrochloric acid, Sigma) to measure residual focal hemosiderin accumulation after hemorrhage. Another series of sections with 400 μm intervals were used to digitize the mRFP-positive pyramidal neurons using fluorescent microscopy in the bilateral cortices. The cervical enlargement (C4-C7) was processed for consecutive vibratome sections, which were scanned with a confocal imaging system to digitize YFP positive CST axons in both sides of the spinal gray matter (Liu et al., 2011; Liu et al., 2009).

Cell culture of embryonic cortical neurons

Cortical neurons were harvested from pregnant female CST-YFP mice at embryonic day 18. Briefly, embryos were removed under deep Ketamine anesthesia, and then the cerebral cortices were dissected and dissociated in Ca^{2+} and Mg^{2+} free Hanks balance salt solution (HBSS, Thermo Fisher Scientific Inc, Wayne, MI) containing 0.125% trypsin (Thermo Fisher Scientific Inc) digestion for 20 minutes, then mechanically triturated for ~20 times. The cells were filtered with a 40 μm cell strainers (BD Falcon, Bedford, MA), and then were seeded onto myelin (10 μg/ml, Sigma St. Louis, MO) and Poly-D-lysine (1 mg/ml, Sigma) coated 24-well plates at a YFP-neuron density of 5000/well in Dulbecco's Modified Eagle's Medium (DMEM; Gibco, Grand Island, NY) containing 5% fetal bovine serum (FBS; Gibco) for 4–6 hours, then changed to neurobasal growth medium (Thermo Fisher Scientific Inc) containing 2% B-27 (Thermo Fisher Scientific Inc), 2 mM GlutaMax (Thermo Fisher Scientific Inc), 2% FBS (Gibco) and 1% antibiotic-antimycotic (Thermo Fisher Scientific Inc) in a moist incubator at 37°C with 5% CO_2. Five different concentrations of tPA (0.065μg/ml, 0.65 μg/ml, 2 μg/ml, 6.5 μg/ml, 13 μg/ml; Genentech Inc, San Francisco, CA) were added to five groups of experiment media and another control group was without tPA.

After 3 days in culture, the cells were fixed by 4% paraformaldehyde for quantification of neurite length and branch number. YFP-positive cells were digitized using a 20x objective (Zeiss) via the MicroComputer Imaging Device (MCID) analysis system (Imaging Research, St. Catharines, Ontario, Canada), and analyzed using MCID software for percentage of neurite positive neurons, branch number and neurite length on total 400–600 neurons distributed in 9 random fields per well with five wells per group.

Data analysis and statistics

Lesion volume was measured by NIH ImageJ and presented as a volume percentage of the lesion area compared with the contralesional hemisphere (Swanson et al., 1990). An Olympus FV1200 (Center Valley, PA, USA) laser-scanning confocal imaging system mounted onto an Olympus Bax 40 microscope was used to digitize the mRFP positive pyramidal neurons in the bilateral cerebral cortices and YFP-labeled CST axons on the cervical cord. The number of PRV-positive neurons in the ipsilateral or contralateral cortex were counted on each one of 5 brain consecutive coronal sections (total 6 sections for each animal), and the data were presented at a series of 0.5 mm interval distances to bregma caudal-rostral, as well as a sum for each hemisphere. The midline of the spinal cord was defined by the central canal on spinal transverse sections. CST axonal density in each side of the spinal gray matter was measured by YFP positive area using NIH ImageJ software on 30 consecutive sections, and the percentage of CST density in the stroke-impaired side to the contralateral side on the same sections was calculated, in order to avoid potential inter-section differences in fluorescent measurements (Liu et al., 2011; Liu et al., 2009). The average number of relative percentage of CST density in each animal was used as an index for CST axonal remodeling after stroke and treatment.

Data are expressed as the mean±SE. Differences of behavioral recovery, numbers of RFP-positive pyramidal neurons, index of axonal density, neurite length and branch number between groups were determined by one-way analysis of variance (ANOVA). Response surface (RS) regression model was used to identify an optimal dose for each response (branch or length grow). Two sample t-test was used to study the lesion difference between the two groups, and Pearson correlation coefficients were calculated to study the correlation of lesion size and functional recovery. A treatment by time interaction was tested to determine whether the tPA treatment effect depended on the time of follow-up assessment. To test the correlation between behavioral outcome and neuronal remodeling after stroke, the Pearson's correlation coefficients between the impaired left forepaw motor performance at 28 days after MCAo and the number of RFP-positive cortical neurons and the index of axonal remodeling in the cervical cord were calculated. A value of $P<0.05$ was considered significant.

Results

Subacute intranasal tPA improves neurological recovery after MCAo

The mean lesion size was comparable in the tPA treated group compared to controls (16.5% vs. 17.7%, p=0.64). Subacute administration of intranasal tPA did not lead to animal death or brain hemorrhage. The neurologic functional status monitored by behavioral tests

suggested comparable severe deficits after MCAo in both animal groups (no difference between groups for either functional test, $p>0.05$), followed by gradual improvement with time thereafter (Figure 1). A significant time dependent improvement was detected using a generalized linear model analysis in the adhesive-removal test ($p<0.001$, A), but not in the single pellet reaching test, although it was marginally significant ($p=0.09$, B). Comparisons between groups displayed a trend that mice receiving tPA treatment demonstrated better behavioral performance one week after the intervention than those that received saline. The difference began to exhibit statistical significance two weeks after treatment in both the unskilled task (i.e. adhesive-removal task, $p<0.05$, A) and the skilled task (i.e. single-pellet reaching test, $p<0.05$, B). These results suggest that intranasal tPA improves functional recovery in MCAo mice in the subacute phase, although tPA treatment did not significantly reduce the lesion volume.

CST axonal remodeling in the denervated side of the cervical cord

In CST-YFP mice, the CST axons on the transverse sections were visible under a laser confocal fluorescence microscope (Liu et al., 2009) (Figure 2). We measured axonal density in the central area of the cervical gray matter in mice stroke models 32 days after right unilateral MCAo. As noted above, we calculated the ratio of CST density in the impaired side to the intact side on the same sections to assess the axonal remodeling in the cervical cord, in order to avoid potential inter-section differences in fluorescent measurements. Data showed that the axonal density in the denervated side of a stroke animal was decreased (B, C) compared to a normal control (A). At 32 days after MCAo, there was a significant increase of CST density in the stroke-impaired side of the cervical cord of tPA-treated mice (C) compared to the saline-treated stroke controls (B, D; $p=0.002$; $F=9.961$), and axons crossing the midline into the impaired side from the intact side were evident in the tPA-treated animals.

Corticospinal innervation originating from bilateral cortices

In order to identify the source of tPA treatment induced CST axonal remodeling in the denervated spinal gray matter, we injected trans-synaptic tracer PRV-614-RFP into the stroke-impaired left forelimb muscles to retrogradely label the neural pathways from the peripheral tissue to the motor cortices in stroke mice. Consistent with previous data (Liu et al., 2009), PRV-positive pyramidal neurons were primarily found in layer V of the motor areas in the right cerebral cortex (Figure 3), while a few neurons with fluorescent labeling could be found in the symmetrical areas in the contralateral hemisphere (B). After stroke, the PRV labeled neurons were dramatically reduced in the ipsilesional cortex (C), but moderately increased in the contralesional cortex (D). The numbers of PRV-positive neurons were higher in both ipsilesional and contralesional cortices of stroke mice treated with intranasal tPA (E and F), compared to those administered with saline (C and D). Table 2 presents the detailed numbers of PRV-positive pyramidal neurons in bilateral cortices on each one of five 100 μm-thick coronal sections of rostral forebrain. The data show that the numbers of PRV-labeled neurons, which reflects the extent of synaptic connection between the stroke impaired forelimb and the motor centers in cortices of both hemispheres, were significantly increased after subacute intranasal tPA treatment, compared with the numbers in mice treated with saline in all caudal forelimb areas (−0.5~0.5 mm rostral to the bregma)

and most rostral forelimb areas (1.5~2.0 mm rostral to the bregma) ($F=44.523$, $p<0.001$ in the ipsilesional hemisphere; $F=9.524$, $p<0.01$ in the contralesional hemisphere; Table 1).

Correlation between functional recovery and neuronal remodeling

The results of Pearson's correlation test showed that animals' behavioral performance measured by both the single-pellet reaching test ($r=0.51$, $p=0.031$) and the adhesive-removal test ($r=-0.60$, $p=0.008$) was significantly correlated with the index of axonal density in the denervated spinal cord (percentage of CST density in the impaired side to the intact side) 32 days after MCAo. There was also a significant correlation between neurological function and number of PRV-positive neurons in the ipsilesional (right) cortex (single-pellet reaching test: $r=0.487$, $p=0.040$; adhesive-removal task: $r=-0.518$, $p=0.028$). No significant correlation was found between either behavior outcome and the number of PRV-positive cells in the contralesional (left) cortex ($p>0.05$), although the statistical analysis suggested a marginal negative correlation between neuron number in the left cortex and the time of adhesive-removal task ($p=0.051$).

PA promotes neurite outgrowth in cultured cortical neurons

To determine the effect of tPA on neurite outgrowth, we compared primary cultured cortical neurons harvested from CST-YFP embryos, using media with five different concentrations of tPA or without tPA. Compared to neurons cultured in media without tPA (Figure 4), the YFP-neurons in tPA media containing tPA at four concentrations (0.65 μg/ml, 2 μg/ml, 6.5 μg/ml and 13 μg/ml; C-F) all exhibited significantly increased neurite outgrowth measured in neurite lengths and number of branches per neuron after 3 days in culture, with a peak at 6.5 μg/ml ($p<0.05$, Table 2). The mean neurite length of neurons in the lowest concentration of tPA medium (0.065 μg/ml) (B) was also significantly longer than that of neurons cultured without tPA ($p<0.01$), while there was no significant difference in branch number between the two groups ($p>0.05$, Table 2). A positive association of dose with length and branch were detected for 0 to 6.5 μg/ml of tPA, but the benefit of high dose was reduced for samples treated with 13 μg/ml of drug. The regression model yielded an estimated optimal dose of 7.58 μg/ml of tPA to achieve average length 496.42 μm and the dose of 7.15 μg/ml to achieve the branch numbers of 8.87. Comparison between the groups: neurite length per neuron $F=17.083$, $p<0.001$; Branch number per neuron $F=10.848$, $p<0.001$.

Discussion

Recombinant tPA is a globally used thrombolytic agent for acute ischemic stroke. In addition to its well established fibrinolytic action, tPA is also involved in synaptic plasticity (Samson and Medcalf, 2006), dendritic remodeling during development (Mataga et al., 2004), and axonal outgrowth after injury (Minor et al., 2009) which may contribute to neural repair. Our previous study in young adult rats demonstrated that intranasal tPA administration during the subacute phase improves neurological recovery after stroke (Liu et al., 2012). In the present study, we further investigated how delayed intranasal tPA promoted neurorestoration. The in vitro data demonstrated that exogenous tPA added to the media in culture chambers promoted neurite outgrowth (neurite length and branch number). Some studies have reported that tPA at a high concentration greater than 200 nM (13 μg/ml) may

potentiate the excitotoxic injury, while at lower concentration it could protect neurons (Nicole et al., 2001; Wu et al., 2013). Our preliminary experiment also showed that medium containing a high concentration of tPA (20 μg/ml) was toxic to neurons (data not shown). Therefore, in the current experiment, we used five test concentrations of tPA less than 20 μg /ml (0.065 μg/ml to 13 μg/ml). The results suggested a dose-dependent trend in neurite outgrowth, and an estimated optimal tPA dose in this culture as 7 to 8 μg/ml. This result is in agreement with prior studies, which suggested both endogenous neuronal tPA and exogenous tPA could contribute to axonal outgrowth (Qian et al., 2016; Xin et al., 2010). These results have led us to postulate the hypothesis that tPA delivered into the CNS facilitates CST axonal sprouting and outgrowth, and thereby restores the corticospinal innervation disrupted by stroke.

The catalytic activity of tPA is rapidly inactivated through the binding of protein inhibitors, primarily plasminogen activator inhibitor-I (PAI-1). The tPA/PAI-1 complex is cleared from the circulation by the liver. Therefore, tPA has a short half-life of 5 to 10 min in the bloodstream. To avoid this rapid inactivation and clearance, we administered tPA by intranasal delivery in mice after stroke. The intranasal method has been demonstrated to directly target the brain and spinal cord along olfactory and trigeminal nerves innervating the nasal passages (Dhuria et al., 2010) and the rostral migratory stream (Scranton et al., 2011) to bypass the blood-brain barrier. Our previous study showed tPA at a dose of 600 μg intranasally could improve the functional recovery and axonal remodeling after stroke in rats (Liu et al., 2012). To determine the efficiency of intranasal delivery, our previous study investigated tPA content in tPA knockout mice treated intranasally with 300 μg recombinant human tPA using a Human tPA Total Antigen ELISA Assay kit (Liu et al., 2012). The concentrations of tPA were 307±10 ng/ml and 228±67 ng/ml at 30 min and 120 min in tPA knockout mice with intranasal treatment, respectively, indicating that intranasal delivery effectively delivers tPA into the brain. To determine distribution of exogenous tPA in the brain, we intranasally delivered 60 μg FITC-labeled human tPA (HTPA-FITC, Molecular Innovations) to C57BL6 mice. Animals were sacrificed 30 min later. Brains were processed for vibratome sagittal sections (100 μm), which were nuclear-stained with DAPI. Our data demonstrate that FITC-labeled tPA was detected as early as 30 min after intranasal delivery in the olfactory bulb, and was widespread in brain regions including the cortex, striatum, subventricular zone (SVZ), DG and CA3 region of hippocampus, thalamus, cerebellum, and brain stem (Supplemental Figure I), which is in good agreement with the rapid tracer distribution study after intranasal delivery (Lochhead et al., 2015).

Since intranasal delivery directly targets the brain, and does not involve systemic delivery, the dose conversion from rats to mice was scaled to the smaller brain size and nasal cavity volumes in mice, i.e., only 1/3-1/2 of that in rats (Gross et al., 1982; Paxinos and Franklin, 1997; Paxinos and Watsson, 1986), instead of the difference of body weight. Seven to 14 days after the stroke is the initiation and maintenance phase of axonal sprouting response (Carmichael, 2006). The potential adverse side effects of tPA may aggravate stroke injury and offset the therapeutic benefits when tPA is applied intravascularly early after stroke. Therefore, to avoid the potential side effects on brain edema and hemorrhagic transformation during the early stage of ischemic onset, we administered tPA intranasally in the period between 7 and 14 days after stroke. As an exploratory proof-of-principle study, we only

examined a single dose of 300 μg tPA with multiple administrations. A dose response study is warranted in the future.

In a series of experiments, we have found that functional recovery after stroke was highly correlated with CST axonal remodeling (Liu et al., 2009), and we have confirmed the direct contribution of the CST to motor behavioral recovery by eliminating the CST axons in the spinal cord with bilateral pyramidotomy (BPT) (Liu et al., 2013). In the in-vivo part of the current study, we evaluate MCAo mice treated with subacute intranasal administration of tPA, and provide data consistent with prior studies of intranasal tPA treatment of ischemic stroke in a rat stroke model (Liu et al., 2012), that subacute intranasal tPA significantly improves neurological recovery in stroke mice, and that the treatment effect depends on the time of follow-up assessment. Intranasal tPA also improved CST recovery in the denervated side of the cervical spinal cord and the pyramidal neuronal reorganization in bilateral cortices. Both skilled and unskilled behavioral recovery during the subacute phase of ischemic stroke are highly correlated with the CST axonal remodeling and the neuronal rewiring to the ipsilesional motor cortex, and recovery is marginally related to neuronal change in the contralesional intact cortex. Combining these results, we speculate that intranasal administration of tPA in the subacute phase after ischemic stroke in adult mice improves neurological functional recovery, at least in part, by neuronal remodeling.

This effect is independent of tPA's ability to cleave plasminogen into plasmin, since no significant difference was found in brain lesion volume between groups, and no significant correlation was found between lesion size and neurological deficit score neither. Neurological improvement may be attributed to CST axonal remodeling in the denervated spinal gray matter originating from both sides of the sensorimotor cortex in the subacute and chronic phase of stroke.

For decades, the primary approach and goal of therapy for stroke has focused on reducing the volume of cerebral infarction and salvaging ischemic neurons in the brain from irreversible injury; however, most efforts have failed to demonstrate efficacy in clinical trials of stroke (Rother, 2008). Therefore, we focused our research efforts on neurorestoration, and our findings provide robust support that subacute intranasal administration of tPA induces neuronal plasticity to compensate for the damaged tissue which thereby enhances functional recovery after stroke. In the current study, we combined transgenic labeling and retrograde viral tracing, in order to comprehensively and directly demonstrate the axonal changes related to functional recovery of the impaired limb. In the CST-YFP mice YFP expression is limited to the forebrain and CST (Bareyre et al., 2005; Liu et al., 2013; Liu et al., 2009). Therefore the labeling in CST-YFP mice is invariable and sensitive. Additionally, PRV is a retrograde trans-synaptic tracer that expresses monomeric red fluorescent protein (RFP) (Banfield et al., 2003). Trans-synaptic transport of the attenuated Bartha strain of PRV between CNS neurons occurs only at points of synaptic contact and proceeds in the retrograde direction (i.e. from postsynaptic to presynaptic neuron). The virus replicates in the infected neurons and infectious particles are released and taken up at synapses, thus spreading along neuronal hierarchical chains (Pickard et al., 2002). Therefore, the PRV labeled neuronal pathways between the motor cortex and the stroke-impaired forelimb are the pathways having substantial synaptic connections re-established by axonal remodeling or

rescued from the ischemic lesion, and not only axonal sprouting. Importantly, such synaptic connections must be effective to allow neuronal signal transmission for motor functional recovery after stroke. By measuring the PRV labeling within the ischemic and contralesional cortex, we are able to assess whether the tPA-induced neuronal reorganization between bilateral hemispheres contribute to functional recovery. In our study, high correlations between functional outcome and CST density index and PRV-positive cortical neurons suggest that the effect of intranasal tPA on behavioral recovery after stroke is attributed to CST axonal remodeling mainly originating from the ipsilesional cortex. The present study was designed to specifically focused on the effects of tPA on CST axonal remodeling. However, we do not exclude the possibility that tPA may also effect CNS parenchymal and vascular cells and further investigation in this area is warranted.

Conclusions

The present study indicates that subacute intranasal administration of tPA significantly enhances behavioral outcome after ischemic stroke, as well as increases CST axonal remodeling in the denervated side of the spinal gray matter and synaptic rewiring of the corticospinal innervation in adult mice. These findings are supported by our in vitro data that tPA dose-dependently increases neurite outgrowth and branching of primary cultured mouse embryonic cortical neurons. Our study suggests that tPA delivered into the brain parenchymal tissue during the subacute phase post stroke may provide efficient neurorestorative effects on neurological recovery.

Supplementary Material

Refer to Web version on PubMed Central for supplementary material.

Acknowledgments

The authors thank Fengjie Wang and Xia Shang for technical assistance.

Sources of Funding

This work was supported by the National Institutes of Neurological Disorders and Stroke (NINDS) of the National Institutes of Health under award number R01NS088656 (MC), American Heart Association Grant 15GRNT25560025 (ZL), and National Natural Science Foundation of China Grant number 81500959 (NC).

References

Banfield BW, Kaufman JD, Randall JA, Pickard GE. Development of pseudorabies virus strains expressing red fluorescent proteins: new tools for multisynaptic labeling applications. J Virol. 2003; 77:10106–10112. [PubMed: 12941921]

Bareyre FM, Kerschensteiner M, Misgeld T, Sanes JR. Transgenic labeling of the corticospinal tract for monitoring axonal responses to spinal cord injury. Nat Med. 2005; 11:1355–1360. [PubMed: 16286922]

Carmichael ST. Cellular and molecular mechanisms of neural repair after stroke: making waves. Ann Neurol. 2006; 59:735–742. [PubMed: 16634041]

Chen J, Li Y, Wang L, Zhang Z, Lu D, Lu M, Chopp M. Therapeutic benefit of intravenous administration of bone marrow stromal cells after cerebral ischemia in rats. Stroke. 2001; 32:1005–1011. [PubMed: 11283404]

Chen J, Zhang C, Jiang H, Li Y, Zhang L, Robin A, Katakowski M, Lu M, Chopp M. Atorvastatin induction of VEGF and BDNF promotes brain plasticity after stroke in mice. J Cereb Blood Flow Metab. 2005; 25:281–290. [PubMed: 15678129]

Dhuria SV 2nd, Hanson LR, Frey WH. Intranasal delivery to the central nervous system: mechanisms and experimental considerations. J Pharm Sci. 2010; 99:1654–1673. [PubMed: 19877171]

Docagne F, Parcq J, Lijnen R, Ali C, Vivien D. Understanding the functions of endogenous and exogenous tissue-type plasminogen activator during stroke. Stroke. 2015; 46:314–320. [PubMed: 25395410]

Farr TD, Whishaw IQ. Quantitative and qualitative impairments in skilled reaching in the mouse (Mus musculus) after a focal motor cortex stroke. Stroke. 2002; 33:1869–1875. [PubMed: 12105368]

Gross EA, Swenberg JA, Fields S, Popp JA. Comparative morphometry of the nasal cavity in rats and mice. J Anat. 1982; 135:83–88. [PubMed: 7130058]

Jauch EC, Saver JL, Adams HP Jr, Bruno A, Connors JJ, Demaerschalk BM, Khatri P, McMullan PW Jr, Qureshi AI, Rosenfield K, Scott PA, Summers DR, Wang DZ, Wintermark M, Yonas H. American Heart Association Stroke, C., Council on Cardiovascular, N., Council on Peripheral Vascular, D., Council on Clinical, C. Guidelines for the early management of patients with acute ischemic stroke: a guideline for healthcare professionals from the American Heart Association/American Stroke Association. Stroke. 2013; 44:870–947. [PubMed: 23370205]

Liu Z, Chopp M, Ding X, Cui Y, Li Y. Axonal remodeling of the corticospinal tract in the spinal cord contributes to voluntary motor recovery after stroke in adult mice. Stroke. 2013; 44:1951–1956. [PubMed: 23696550]

Liu Z, Li Y, Zhang L, Xin H, Cui Y, Hanson LR, Frey WH 2nd, Chopp M. Subacute intranasal administration of tissue plasminogen activator increases functional recovery and axonal remodeling after stroke in rats. Neurobiol Dis. 2012; 45:804–809. [PubMed: 22115941]

Liu Z, Li Y, Zhang RL, Cui Y, Chopp M. Bone marrow stromal cells promote skilled motor recovery and enhance contralesional axonal connections after ischemic stroke in adult mice. Stroke. 2011; 42:740–744. [PubMed: 21307396]

Liu Z, Zhang RL, Li Y, Cui Y, Chopp M. Remodeling of the corticospinal innervation and spontaneous behavioral recovery after ischemic stroke in adult mice. Stroke. 2009; 40:2546–2551. [PubMed: 19478220]

Lochhead JJ, Wolak DJ, Pizzo ME, Thorne RG. Rapid transport within cerebral perivascular spaces underlies widespread tracer distribution in the brain after intranasal administration. J Cereb Blood Flow Metab. 2015; 35:371–381. [PubMed: 25492117]

Mataga N, Mizuguchi Y, Hensch TK. Experience-dependent pruning of dendritic spines in visual cortex by tissue plasminogen activator. Neuron. 2004; 44:1031–1041. [PubMed: 15603745]

Minor K, Phillips J, Seeds NW. Tissue plasminogen activator promotes axonal outgrowth on CNS myelin after conditioned injury. J Neurochem. 2009; 109:706–715. [PubMed: 19220707]

Nicole O, Ali C, Docagne F, Plawinski L, MacKenzie ET, Vivien D, Buisson A. Neuroprotection mediated by glial cell line-derived neurotrophic factor: involvement of a reduction of NMDA-induced calcium influx by the mitogen-activated protein kinase pathway. J Neurosci. 2001; 21:3024–3033. [PubMed: 11312287]

Paxinos, G., Franklin, K. The Mouse Brain in Stereotaxic Coordinates. Academic Press; San Diego: 1997.

Paxinos, G., Watsson, C. The Rat Brain in Stereotaxic Coordinates. Academic Press; San Diego: 1986.

Pickard GE, Smeraski CA, Tomlinson CC, Banfield BW, Kaufman J, Wilcox CL, Enquist LW, Sollars PJ. Intravitreal injection of the attenuated pseudorabies virus PRV Bartha results in infection of the hamster suprachiasmatic nucleus only by retrograde transsynaptic transport via autonomic circuits. J Neurosci. 2002; 22:2701–2710. [PubMed: 11923435]

Powers WJ, Derdeyn CP, Biller J, Coffey CS, Hoh BL, Jauch EC, Johnston KC, Johnston SC, Khalessi AA, Kidwell CS, Meschia JF, Ovbiagele B, Yavagal DR. American Heart Association Stroke, C., 2015. American Heart Association/American Stroke Association Focused Update of the 2013 Guidelines for the Early Management of Patients With Acute Ischemic Stroke Regarding Endovascular Treatment: A Guideline for Healthcare Professionals From the American Heart Association/American Stroke Association. Stroke. 2015; 46:3020–3035. [PubMed: 26123479]

Qian J-Y, Chopp M, Liu Z. Mesenchymal stromal cells promote axonal outgrowth directly and synergistically with astrocytes via tPA. PLoS One. 2016 in press.

Rother J. Neuroprotection does not work! Stroke. 2008; 39:523–524. [PubMed: 18202309]

Samson AL, Medcalf RL. Tissue-type plasminogen activator: a multifaceted modulator of neurotransmission and synaptic plasticity. Neuron. 2006; 50:673–678. [PubMed: 16731507]

Scranton RA, Fletcher L, Sprague S, Jimenez DF, Digicaylioglu M. The rostral migratory stream plays a key role in intranasal delivery of drugs into the CNS. PLoS One. 2011; 6:e18711. [PubMed: 21533252]

Swanson RA, Morton MT, Tsao-Wu G, Savalos RA, Davidson C, Sharp FR. A semiautomated method for measuring brain infarct volume. J Cereb Blood Flow Metab. 1990; 10:290–293. [PubMed: 1689322]

Thorne RG, Pronk GJ, Padmanabhan V, Frey WH 2nd. Delivery of insulin-like growth factor-I to the rat brain and spinal cord along olfactory and trigeminal pathways following intranasal administration. Neuroscience. 2004; 127:481–496. [PubMed: 15262337]

Wu F, Echeverry R, Wu J, An J, Haile WB, Cooper DS, Catano M, Yepes M. Tissue-type plasminogen activator protects neurons from excitotoxin-induced cell death via activation of the ERK1/2-CREB-ATF3 signaling pathway. Mol Cell Neurosci. 2013; 52:9–19. [PubMed: 23063501]

Xin H, Li Y, Shen LH, Liu X, Wang X, Zhang J, Pourabdollah-Nejad DS, Zhang C, Zhang L, Jiang H, Zhang ZG, Chopp M. Increasing tPA activity in astrocytes induced by multipotent mesenchymal stromal cells facilitate neurite outgrowth after stroke in the mouse. PLoS One. 2010; 5:e9027. [PubMed: 20140248]

Zai L, Ferrari C, Dice C, Subbaiah S, Havton LA, Coppola G, Geschwind D, Irwin N, Huebner E, Strittmatter SM, Benowitz LI. Inosine augments the effects of a Nogo receptor blocker and of environmental enrichment to restore skilled forelimb use after stroke. J Neurosci. 2011; 31:5977–5988. [PubMed: 21508223]

Highlights

- Subacute intranasal tPA treatment promotes behavioral outcome after stroke
- CST axonal remodeling mainly originates from the ipsilesional cortex
- tPA increases neurite outgrowth and branching of primary cortical neurons
- tPA in the brain parenchymal tissue provides efficient neurorestorative effects

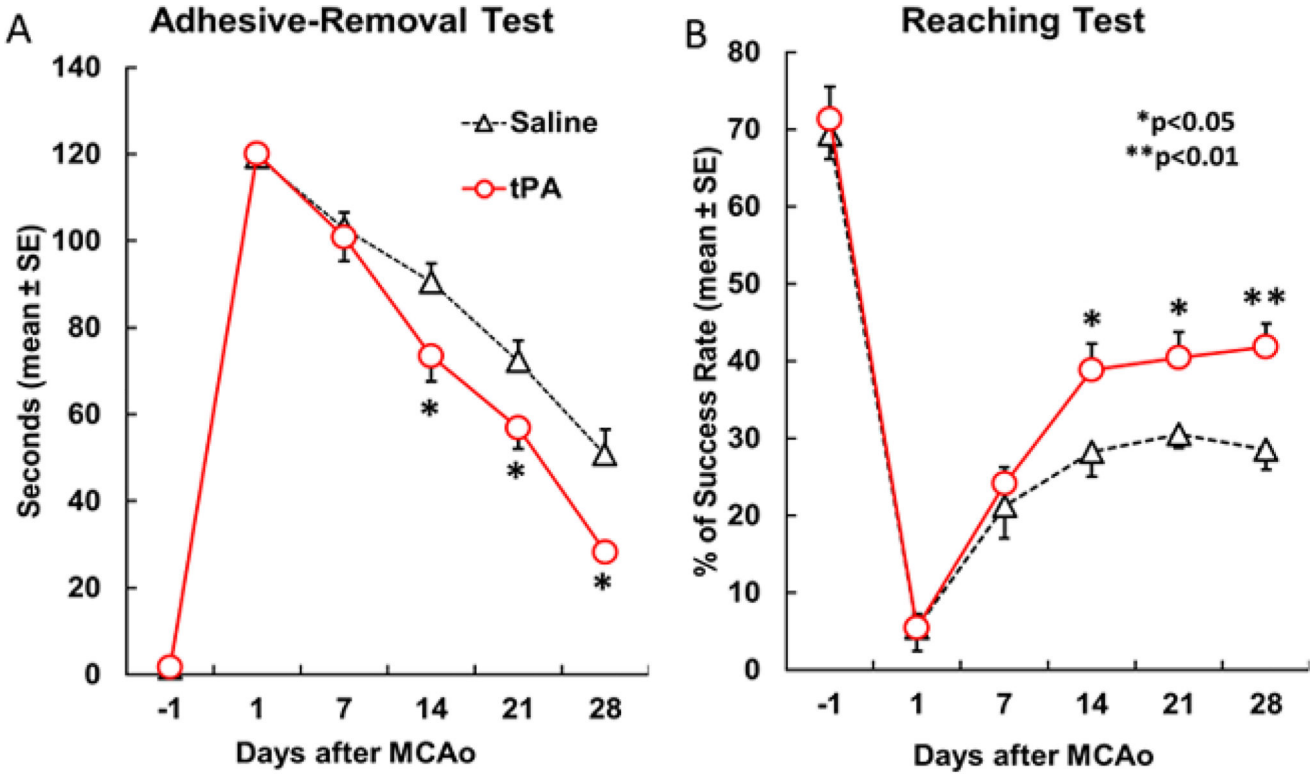

Figure 1.

Temporal profile of the left forepaw deficit and recovery after right MCAo assessed with adhesive-remove test (A) and single pellet reaching test (B). Note that significant behavioral deficits and progressive recovery were observed with both tests in all mice; while subacute tPA intranasal treatment significantly enhanced functional recovery compared with saline treated mice (n=10/group, $p<0.05$ vs control).

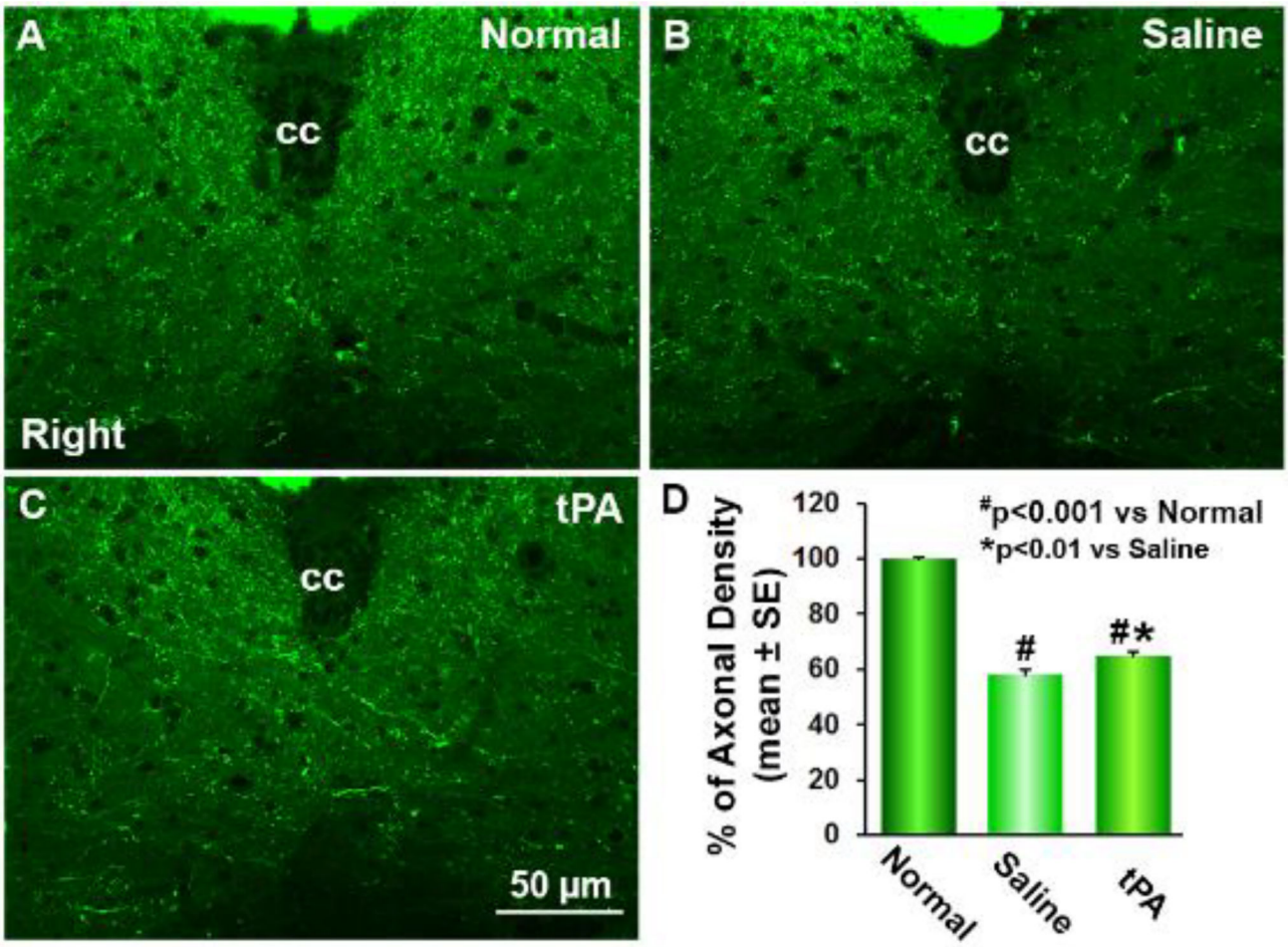

Figure 2.

Single layer confocal images of gray matter of the cervical cord. In transgenic CST-YFP mice, the CST axons are fluorescent yellow-green under a laser-scanning confocal microscopy (A-C). Thirty-two days after right MCAo, compared to normal mice (A), YFP-positive CST axonal density was reduced in the denervated side of the cervical gray matter (B and C), while axons crossing the midline into the denervated left side from the right intact side were evident in the tPA treated mice (C). Quantitative analysis of the percentage of CST axons in the denervated side to the contralateral side demonstrated that intranasal tPA treatment significantly increased axonal density in the denervated gray matter (D, n=10 per group, p<0.0

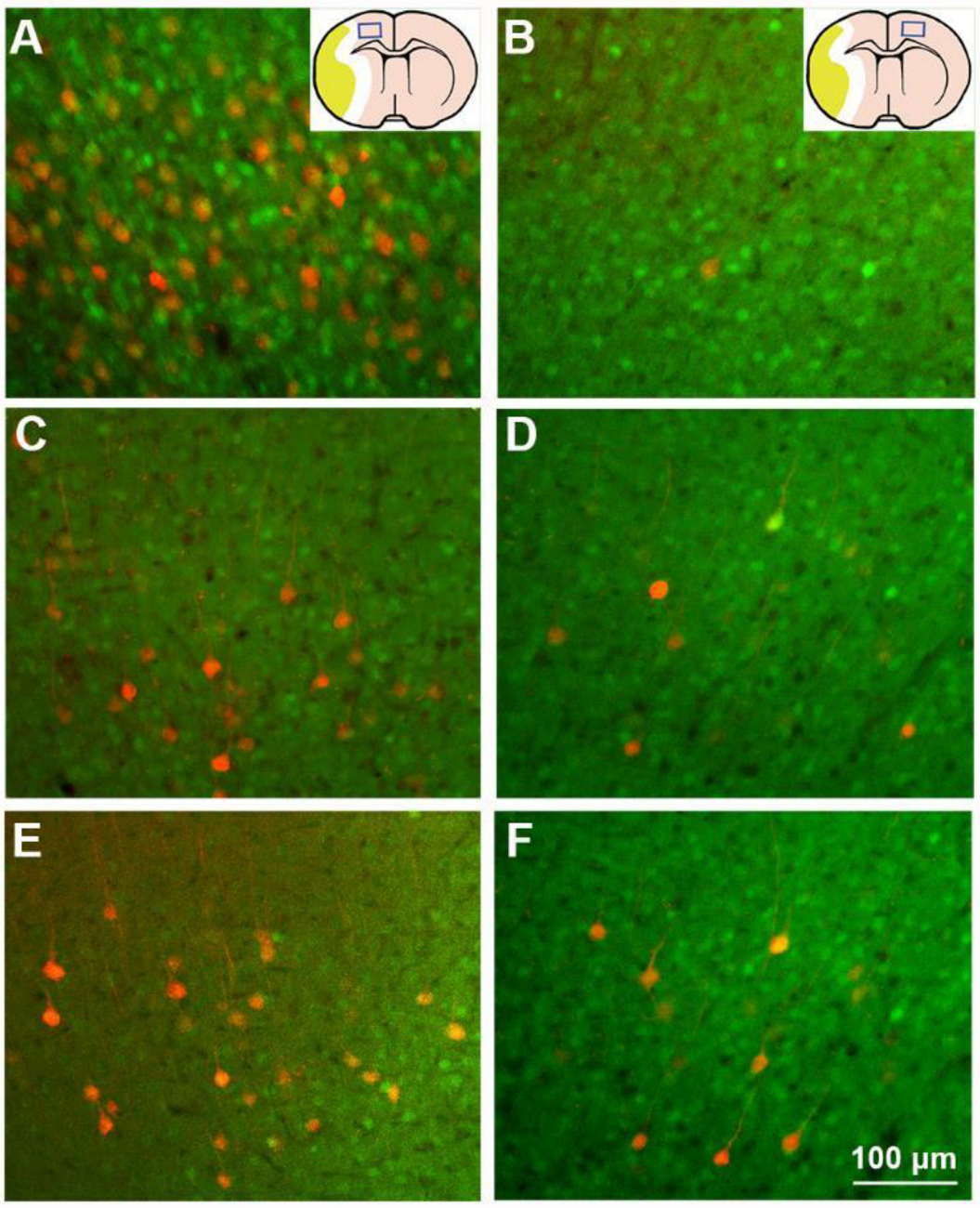

Figure 3.

Single layer fluorescent microscopy images on coronal brain sections at the bregma level. Four days after tracer injection into the left forelimb muscles, PRV labeling was primarily found in the right cortex (A), and rarely in the left cortex (B) in normal mice. In stroke mice, PRV-positive cortical neurons in the right cortex were dramatically reduced (C), while PRV-labeled cells in the left contralesional cortex was comparable with normal mice (D). In contrast, intranasal tPA treatment increased the PRV labeling in both ipsilesional (E) and contralesional hemispheres (F) compared with saline treated mice.

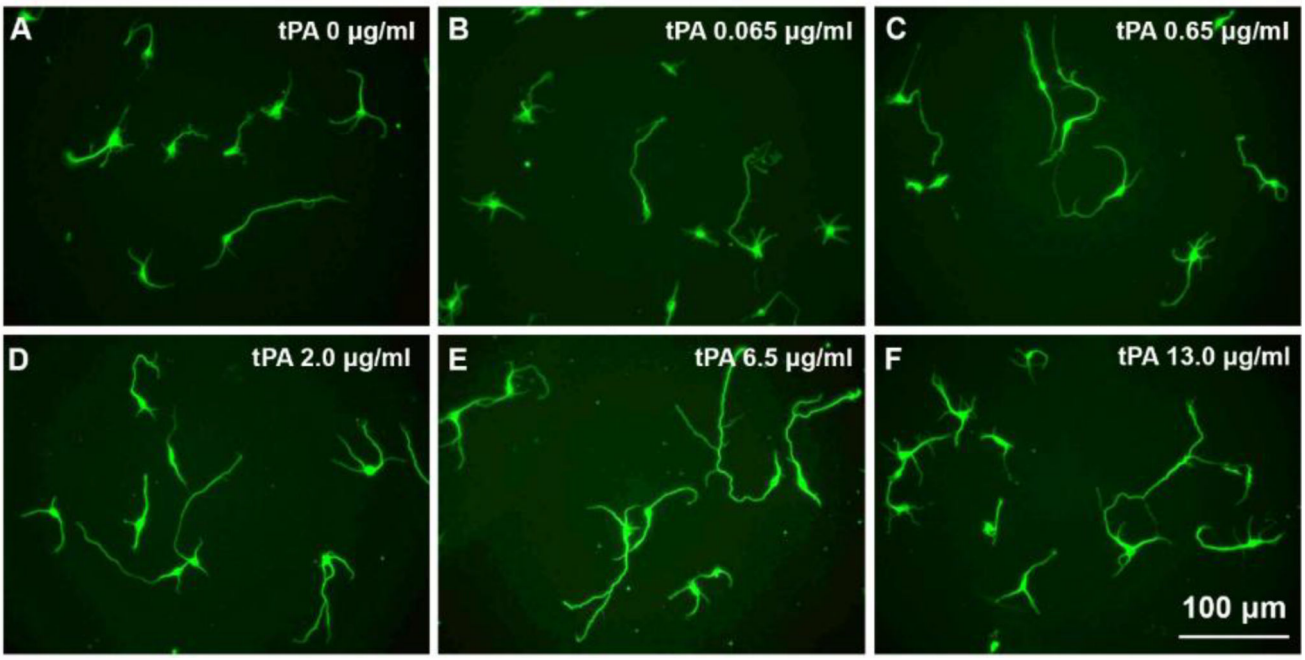

Figure 4.

Representative images show cortical neurons isolated from embryos of CST-YFP mice cultured with different concentrations of tPA (A-F, 0 to 13 μg/ml). Note that both neurite length and branch numbers were increased with concentration of tPA, and reached a peak at 6.5 μg/ml.

Table 1

Numbers of RFP-positive pyramidal neurons in the bilateral cortices.

Groups		mm to bregma						Total
		−0.5	**0**	**0.5**	**1.0**	**1.5**	**2.0**	
Normal	Right	81.2±2.9	134.0±3.5	19.0±1.4	2.7±0.8	24.2±1.8	30.5±2.0	291.5±7.0
	Left	2.0±0.4	5.7±0.8	0.3±0.3	0.3±0.3	3.5±0.9	3.3±0.4	15.2±1.3
Saline	Right	30.4±4.5	73.1±2.8	21.0±3.3	4.2±0.4	16.7±1.4	15.7±2.7	161.1±6.7
	Left	8.7±1.1	17.7±2.2	8.4±0.9	3.7±0.6	10.0±0.9	7.4±0.6	55.9±3.2
tPA	Right	48.0±1.3**	95.7±5.3**	33.1±3.4*	8.3±1.0**	23.0±2.9	26.0±2.9*	234.1±7.9***
	Left	20.3±3.7*	28.6±4.2*	16.1±1.5**	6.0±1.0	13.3±2.2	8.8±0.5	93.1±11.0**

Numbers are mean±SE.

* $p<0.05$

** $p<0.01$

*** $p<0.001$ vs Saline treated group (n=10/group).

Table 2

tPA enhanced neurite outgrowth and branching of primary cultured embryonic cortical neurons from CST-YFP mice.

tPA (μg/ml)	0	0.065	0.65	2.0	6.5	13.0
Neurite length per neuron (μm)	330.4±8.3	371.6±15.5 **	417.5±11.5 ***	433.0±14.6 ***	483.9±4.2 ***	432.9±6.7 ***
Branch number per neuron	6.69±0.27	6.78±0.35	7.98±0.13 ***	7.95±0.10 **	8.72±0.16 ***	7.68±0.46 *

Numbers are mean ± SE.

* p<0.05

** p<0.01

*** p<0.001 vs. Saline treated group.